Published in final edited form as:

Neuron. 2019 May 08; 102(3): 564–573.e6. doi:10.1016/j.neuron.2019.02.029.

Pain-Induced Negative Affect Is Mediated Via Recruitment Of The Nucleus Accumbens Kappa Opioid System

Nicolas Massaly[1], **Bryan A. Copits**[1], **Adrianne R. Wilson-Poe**[1], **Lucia Hipólito**[2], **Tamara Markovic**[1], **Hye Jean Yoon**[1], **Shiwei Liu**[3], **Marie C. Walicki**[1,4,5], **Dionnet L. Bhatti**[1], **Sunil Sirohi**[6], **Amanda Klaas**[7], **Brendan M. Walker**[6], **Rachael Neve**[8], **Catherine M. Cahill**[3], **Kooresh I. Shoghi**[7,9], **Robert W. Gereau IV**[1,9], **Jordan G. McCall**[1,4,5], **Ream Al-Hasani**[1,4,5,#], **Michael R. Bruchas**[1,9,#], and **Jose A. Morón**[1,9,#,*]

[1]Department of Anesthesiology; Washington University Pain Center; Washington University in St. Louis; School of Medicine; St. Louis, MO, 63110; USA

[2]Department of Pharmacy and Pharmaceutical Technology and Parasitology; University of Valencia; Valencia, 46100; Spain

[3]Department of Psychiatry and Biobehavioural Sciences; University of California; Los Angeles, CA, 90095; USA

[4]Department of Pharmaceutical and Administrative Sciences; St. Louis College of Pharmacy; St. Louis, MO, 63110 ; USA

[5]Center for Clinical Pharmacology; St. Louis College of Pharmacy and Washington University in St. Louis School of Medicine ; St. Louis, MO, 63110 ; USA

[6]Department of Psychology; Washington State University; Pullman, WA, 99164-4820; USA

[7]Department of Radiology; Washington University in St. Louis; School of Medicine; St. Louis, MO, 63110 ; USA

[8]Department of Brain and Cognitive Science; Viral Gene Transfer Core, M.I.T.; Cambridge, MA, 02139-4307; USA

[9]Department of Neuroscience; Washington University in St. Louis; St. Louis, MO, 63110 ; USA

SUMMARY

[#]Co-corresponding Authors : Ream Al-Hasani (al-hasanir@wustl.edu), Michael R. Bruchas (mbruchas@uw.edu) and Jose A. Morón (jmoron-concepcion@wustl.edu).

AUTHORS CONTRIBUTIONS

Conceptualization, N.M., L.H., R W.G., K.S., R.A, M.R.B., and J.A.M.; Methodology, N.M., R.A, M. R.B., and J.A.M.; Formal analysis, N.M., and J.A.M.; Investigation, N.M., B.C., A.W-P., M.C.W., J.G.M., T.M., L.H., H.J. Y., B.M.W., S.S., L.S., C.M.C., D.L.B., and R.A.; Writing - Original Draft, N. M., R.A., M.R.B., and J.A.M.; Writing – Review & Editing, N.M., R.A., M.R.B., and J.A.M.; Funding Acquisition : R.A., M.R.B., and J.A.M.; Resources, R.N., R.A., M.R.B., and J.A.M.; Supervision, N.M., R.A., M.R.B., and J.A.M.

[*]Lead Contact ; Jose A. Morón: jmoron-concepcion@wustl.edu

DECLARATION OF INTERESTS

The authors declare no competing financial interests.

Negative affective states impact quality of life for patients suffering from pain. These maladaptive emotional states can lead to involuntary opioid overdose, and many neuropsychiatric comorbidities. Uncovering the mechanisms responsible for pain-induced negative affect is critical in addressing these comorbid outcomes. The nucleus accumbens (NAc) shell, which integrates the aversive and rewarding valence of stimuli, exhibits plastic adaptations in the presence of pain. In discrete regions of the NAc, activation of the kappa opioid receptor (KOR) decreases the reinforcing properties of rewards and induces aversive behaviors. Using complementary techniques we report that *in vivo* recruitment of NAc shell dynorphin neurons, acting through KOR, is necessary and sufficient to drive pain-induced negative affect. Taken together, our results provide evidence that pain-induced adaptations in the kappa opioid system within the NAc shell represent a functional target for therapeutic intervention that could circumvent pain-induced affective disorders.

Graphical Absract

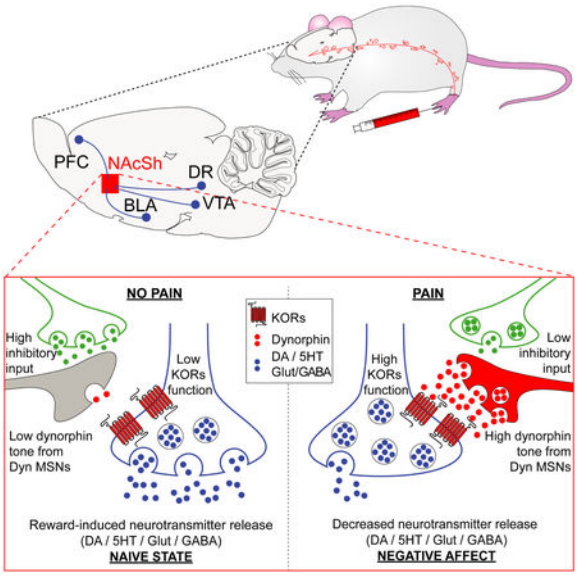

eTOC

In the current manuscript Massaly et al., identify a pain-induced enhancement in the kappa opioid system within nucleus accumbens, which drives pain-associated negative emotional states. These results provide a functional substrate for therapies that would circumvent pain-induced affective disorders.

INTRODUCTION

Pain is a major, growing epidemic in the U.S., afflicting more than 30% of the population (Elman et al., 2013). In this maladaptive condition, the presence of under- or untreated negative affective states largely drives anxiety- / stress-induced disorders and involuntary opioid overdoses (Elman and Borsook, 2016; Volkow and McLellan, 2016). Despite the drive to improve pain treatment and prevent tragic outcomes, the mechanisms underlying these negative affective states are not yet clear. Recent human studies show reduced nucleus

accumbens (NAc) activity, alterations in reward evaluation, decision making, and motivation in pain patients (Apkarian et al., 2004; Verdejo-García et al., 2009). In rodent models, transient activation of kappa opioid receptors (KORs) in a discrete sub-region of the NAc abates the reinforcing and motivational values of rewards through presynaptic inhibition of dopamine, glutamate and serotonin release (Crowley and Kash, 2015; Narita et al., 2005; Tejeda et al., 2017). This behavioral adaptation is also observed during inflammatory pain, which represents a characteristic feature of negative affective states (Al-Hasani et al., 2015; Castro and Berridge, 2014; Narita et al., 2005; Shippenberg et al., 1988; Verdejo-García et al., 2009). We hypothesized that KORs in a sub-region of the NAc (NAc shell cold spot: NAcShCS for rats and ventro-medial NAc shell: vNAcSh for mice) represent a key mechanism for generating pain-induced negative affective states.

RESULTS

Kappa opioid receptors are both necessary and sufficient to drive pain-induced negative affect

Recent evidence from pain and depression studies report that decreased motivation in goal-directed behavior represents a characteristic feature of pain-induced negative affect (Hipólito et al., 2015; Schwartz et al., 2014). Therefore, to determine the role of the KORs in these maladaptive states, we combined local microinjection of the long-acting selective KOR antagonist, norbinaltorphimine (norBNI), with a progressive ratio (PR) schedule of reinforcement for sucrose rewards (Figure 1A). In agreement with previous literature (Leitl et al., 2014; Narita et al., 2005; Schwartz et al., 2014) inflammatory pain decreased the motivational state of rats as measured by a lower number of rewards earned (Figure 1B-C) . Local pharmacological blockade of KORs, using bilateral micro-injections of norBNI (2 μg/side) into the NAcShCS, was sufficient to prevent this pain-induced decrease in motivation (Figure 1B-C). This result cannot be attributed to an intrinsic effect of norBNI as blockade of KORs alone, in sham-pain conditions, did not alter the rat's motivational state (norBNI-Saline - Figure 1B-C). Furthermore, inflamed rats did not exhibit any difference in reward acquisition when lower efforts were required (i.e. the initial slope of reward earning during PR test (Figure 1C) or in a fixed ratio schedule of reinforcement (Hipólito et al., 2015)). This demonstrates that inflammatory pain did not affect the ability for rats to interact with the reward-paired lever, but rather impaired their motivation when high efforts were required to obtain the reward. Additionally, while injection of norBNI in the NAcShCS reversed pain-induced negative affective state, CFA-induced hyperalgesia, measured using Hargreaves thermal test, was not impacted (Figure 1D). These results demonstrate that KOR blockade in the NAcShCS reverses pain-induced negative affective states without affecting thermal hyperalgesia. It has been widely shown that pain-induced decrease in motivated behavior occur across species (Okun et al., 2016; Schwartz et al., 2014). Therefore, to determine the extent to which these findings apply to other species, we conducted additional studies to further evaluate a potential role for KOR in pain-induced negative affect in both male and female mice (Figure 1E-H). Local micro-injection of norBNI (2 μg/side) in the vNAcSh reversed the pain-induced decrease in motivation observed two days after CFA treatment (Figure 1E-H) in both sexes. Importantly, this result emphasizes a KOR-dependent mechanism in the vNAcSh to drive pain-induced negative affect across species and sexes.

Overall, our data suggest that KORs are necessary within the NAcShCS/vNAcSh for reducing motivated behavior induced by inflammatory pain, without directly impacting the nociceptive component of pain (Figure 1B-H). In order to examine whether activation of KOR within the NAc would be sufficient to drive a decrease in motivation, rats received a local bilateral micro-injection of the short-acting KOR agonist, U50,488 (1 μg/side) (Figure 1I). Selective engagement of KOR signaling within the NAcShCS induced a significant decrease in motivation for sucrose self-administration in naïve rats (Figure 1J-K). Moreover, restoration in sucrose seeking was observed during a third PR test ran 24 hours after pharmacological treatment, a time point at which U50,488 is washed off (Figure 1J-K). Interestingly, local KOR stimulation did not impact sucrose self-administration on a fixed ratio schedule of reinforcement nor did it impact the initial shape of the PR test (Figure S1A-C and Figure 1K, respectively). These data further support the specific involvement of KORs in the NAcShCS in decreasing motivated behavior rather than causing a generalizable behavioral impairment.

Activation of dynorphin-containing neurons in the vNAcSh is sufficient to drive negative affective states and aversive behavior

In the NAcSh a large population of MSNs contain dynorphin and locally control pre-synaptic neurotransmitter release (Al-Hasani et al., 2015; Nestler and Carlezon, 2006). To investigate the role of these dynorphin-containing neurons on negative affective states, we selectively expressed channelrhodopsin-2 (ChR2) in the vNAcSh of dynorphin-cre+ mice (Figure 2A). Here we observe that stimulation of dynorphin-containing neurons in the vNAcSh is sufficient to decrease motivation to self-administer sucrose (Figure 2B-D). In addition, we previously reported that stimulation of dynorphin-containing neurons in the vNAcSh was sufficient to drive a KOR-dependent real-time place aversion (RTPA) (Al-Hasani et al., 2015). We combined RTPA-induced photo-stimulation of dynorphin-containing neurons in the vNacSh with local KOR blockade using norBNI (2 μg and 4 μg in 0.5 μl) to test their involvement in mediating negative affective states and aversive behavior during inflammatory pain. We found that local NAc norBNI pre-treatment (2 μg and 4 μg per side) blocks dynorphin-neuron stimulated RTPA (Figure 2E-G). Interestingly, 48 hours after CFA injection, pretreatment with 2 μg of norBNI no longer prevented KOR-mediated aversion (Figure 2F-G). However, local vNAcSh infusion of 4 μg of norBNI blocked the aversion in inflammatory pain conditions. Importantly, KOR blockade did not impact locomotor activity (Figure 2H) nor have an effect on RTPT behavior in eYFP-expressing controls (Figure S1D-F). Furthermore, we demonstrated that norBNI micro-injection in the vNAcSh did not impact the inflammatory pain-induced anxiety as measured in an open field chamber (Figure S1G-I), consistent with a role of KORs in anxiety in the amygdala (Al-Hasani et al., 2015; Bruchas et al., 2009; Crowley et al., 2016; Knoll and Carlezon, 2010). Our results indicate that pain does not potentiate the aversive behavior induced by dynorphin-containing neuron photo-stimulation, they suggest that KORs are required for the modulation of pain-induced negative affect. These findings identify a key role for KOR/dynorphin system in pain-induced negative affect.

Inflammatory pain increases KOR functional activity and recruits dynorphin-containing neurons in the NAcShell through a disinhibition mechanism

In order to determine how inflammatory pain engages the KOR system in the NAcShCS, we used *in situ* hybridization in rat tissue to measure the expression of KOR mRNA (*Oprk1*) (Tejeda et al., 2017). No significant differences in KOR mRNA expression were observed between saline- and CFA-injected animals 48 hours after pain induction (Figure S2A-B). In addition, we assessed KOR functional activity using a radio-labelled non-hydrolysable [^{35}S] GTPγS to measure KOR-dependent G-protein coupling. Dynorphin A-stimulated [^{35}S] GTPγS binding was significantly elevated in the NAc of CFA-injected animals compared to controls (Figure 3A), indicating enhanced KOR G-protein coupling in inflammatory pain. For additional anatomical resolution, we utilized [^{35}S] GTPγS autoradiography in brain slices (Liu et al., 2016). In CFA-injected rats, KOR-induced G-protein activation was enhanced in the NAc shell (Figure 3B-D). This increase was dependent on KOR activation, as no radioactive incorporation was visualized when slices were with both KOR agonist and a selective KOR antagonist. Interestingly, only a slight non-significant increase in [^{35}S] GTPγS radiolabeling was observed in the NAc core and in the band of Broca, suggesting that enhanced KOR-mediated activation of Gα signaling in pain conditions is tightly localized to the NAc shell (Figure 3D). Compensatory changes in the KOR system may also be mediated via recruitment of dynorphin-containing medium spiny neurons (MSNs). We hypothesized that changes in NAc dynorphin tone may underlie the KOR-dependent decrease in motivation and adaptive changes in KOR activity observed during pain (Liu et al., 2016; Muschamp and Carlezon, 2013; Narita et al., 2005). To test this, we examined the expression of the dynorphin A peptide in the NAc shell using immmunohoistochemistry. Rats experiencing inflammatory pain exhibited a robust increase in dynorphin A expression within the NAcShCS (Figure 3E-F) compared to sham-pain controls. To investigate if this increase in dynorphin A expression was correlated with an increase in dynorphin neuron excitability, we conducted whole-cell patch clamp electrophysiological recordings on dynorphin-containing neurons in the vNAcSh in dynorphin-cre+ reporter mice (Figure 3G) (Al-Hasani et al., 2015; Krashes et al., 2014). Dynorphin-containing neurons from CFA-treated reporter mice exhibited enhanced excitability, as measured by a depolarized resting membrane potential and a lower rheobase (Figure 3H-J). These results demonstrate that inflammatory pain significantly increases the excitability of dynorphin-containing vNAcSh neurons (Figure 3H-J). To determine the potential cellular mechanisms underlying this increase in dynorphinergic tone within the NAcSh, we examined spontaneous synaptic input to the vNAcSh using dynorphin-cre reporter mice. In inflammatory pain, as compared to sham-pain controls, a decrease in the frequency and amplitude of spontaneous inhibitory postsynaptic currents was specifically observed in dynorphin-containing neurons (Figure 3K-P). Interestingly, a shift in the distribution towards increased inhibitory tone onto non-dynorphin neurons in vNAcSh was also observed (Figure 3N-P). Together, these results support the conclusion that a pain-induced selective disinhibition of dynorphin-containing neurons leads to an enhancement of their excitability in the vNAcSh.

Inflammatory pain mediates negative affective states through recruitment of dynorphin-containing neurons in the NAcShCS

To further determine whether pain-induced increase in dynorphin cells excitability results in an enhancement in dynorphin tone, we used *in vivo* positron emission tomography (PET) imaging (Figure 4A). In anesthetized rats, the binding efficacy of a radioactive competitive antagonist for KORs, ^{11}C-LY2795050 (Zheng et al., 2013), was measured before (baseline) or 48 hours after a saline or a CFA injection as an indirect measure of receptor occupancy. Compared to baseline, the distribution volume of ^{11}C-LY2795050 was significantly decreased when rats were in pain while it remained unchanged in sham-pain control animals (Figure 4B-C). This selective reduction in ^{11}C-LY2795050 binding suggests an elevation in endogenous dynorphin onto KORs during inflammatory pain.

We then examined whether dynorphin-containing neuronal activation is necessary for the observed effects of inflammatory pain on motivated behavior, using a chemogenetic approach (Roth, 2016) to selectively silence the activity of NAc dynorphin-containing neurons. Following a baseline PR test, wild type rats were bilaterally micro-injected in the NAcShCS with a herpes simplex virus (HSV) containing inhibitory designer receptors exclusively activated by designer drugs (DREADDs) (Dyn2.0-hM4Di-IRES-mCherry) or its control virus (Dyn2.0-IRES-mCherry) (Figure 4D). This approach allowed us to specifically target NAcShCS dynorphin-containing neurons (Figure S3A-B) and decrease their excitability upon CNO administration (Figure S3C-F). Importantly, CNO alone did not impact neuronal excitability (Figure S3G-J). As previously described, rats experiencing inflammatory pain display a significant decrease in motivation compared to sham-pain animals. Chemogenetic silencing of NAcShCS dynorphin-containing neurons blocked the decrease in motivation observed in CFA-treated animals (Figure 4E). Importantly, the sole expression of Gai-coupled DREADDs, not acute CNO administration ($1 mg.kg^{-1}$) impacted pain-induced decrease in motivated behavior (Figure 4E). Lastly, silencing dynorphin-containing neurons did not increase motivated behavior in non-pain conditions (Figure 4E). These results establish that neither DREADD expression nor CNO administration have non-specific actions on these behaviors (Figure 4E). Altogether these results demonstrate that dynorphin-containing neuronal activity is necessary for generating inflammatory pain-induced negative affect.

DISCUSSION

In the present study, we identified a critical role for the kappa opioid system in the modulation of negative affect associated with inflammatory pain. We report that pain enhances dynorphin expression and recruits dynorphin-containing neurons in a discrete subregion of the NAc shell through a disinhibition mechanism. In addition, we further report that pain increases KOR function and occupancy using both GTPγS binding and *in vivo* PET imaging. Finally, using a complementary series of pharmacological, optogenetic, and chemogenetic approaches we report that both dynorphin-containing neurons and KOR activity in the NAc shell are both necessary and sufficient to drive pain-induced negative affective states.

Previous evidence has uncovered a role for the dynorphin peptide in decreasing opioid-mediated goal-directed behaviors and opioid-induced dopamine release in the NAc during pain states (Narita et al., 2005; Verdejo-García et al., 2009). However, the source of endogenous peptide and its consequent mechanism of action have remained elusive. In the current work, we uncover that pain is sufficient to increase dynorphin expression in the NAcShCS (Figure 3E-F) and recruit local dynorphin-containing neuron activity (Figure 3G-I). We determine that this recruitment is due to a substantial decrease in IPSCs onto these NAc dynorphin-containing neurons, leading to an hyper-excitable state for those neurons (Figure 3G-M). We demonstrate for the first time, using PET scan imaging in rodents, that pain induces increases in dynorphin tone *in vivo* (Figure 4A-C). In light of the overall increase in KOR occupancy observed in our study, it is important to consider the possibility that several hubs of dynorphin-containing neurons, such as ventral pallidum or lateral hypothalamus (Baldo et al., 2003; Peyron et al., 1998), are also recruited during pain conditions.

Through the development of a gen 2.0 specific and efficient inhibitory DREADDs (Figure S3) in rats, we uncover the role of the NAcShCS dynorphin-containing neuron recruitment in pain-induced decreases in motivational states (Figure 4D-E). Together these results reveal a source of endogenous dynorphin in the vNAcSh/NAcShCS that drives pain-induced negative affect, resolving an important gap in our understanding of the impact of pain on dynorphin-KOR system.

Recent studies have identified alterations in excitatory transmission onto D2-expressing MSNs in the NAc during inflammatory and neuropathic pain (Ren et al., 2016; Schwartz et al., 2014). While these studies describe increased excitatory inputs (Ren et al., 2016) that can trigger long-term plasticity at synapses onto D2R-expressing neurons (Schwartz et al., 2014), we report here that dynorphin-containing neurons are specifically disinhibited in inflammatory pain (Figure 3K-M). Furthermore, while NAc receives KOR enriched synaptic terminals from brain structures involved in affect and motivation (Bruchas et al., 2009; Land et al., 2009; Margolis et al., 2003; Muschamp and Carlezon, 2013), we demonstrate here that local KOR blockade in the NAc reverses pain-induced negative affect in both mice and rats (Figure 1). Local release of dynorphin, activating KORs in the NAc, may thus negatively regulate the release of serotonin, dopamine, glutamate and/or GABA leading to altered NAc function in pain-induced behaviors including reward seeking. Despite this evidence, the role of other peptides and neurotransmitters in pain-induced negative affect cannot be ignored. Similarly, activation of the KOR system located outside of the NAc may be necessary to drive pain-induced adaptations in negative affect. Nonetheless, in addition to previous reports (Ren et al., 2016; Schwartz et al., 2014), our work provides a novel allostatic mechanism through which pain impacts the nucleus accumbens microcircuitry to induce negative affective states.

Using a combination of pharmacological studies in both rats and mice we show that adaptations in the dynorphin KOR system occur when aversive behaviors are measured in conditions of pain (Figure 2). Lastly, a recent study from Yang and collaborators has uncovered two distinct accumbens shell subregions projecting to the VTA to regulate motivational states (Yang et al., 2018). Future studies will further examine how the

dynorphin-containing neuronal population described in our findings integrates with those specific circuits to drive motivational state adaptations in pain conditions.

While other studies describe a potential therapeutic role for KOR antagonists (Al-Hasani et al., 2015; Castro and Berridge, 2014; Chavkin, 2011), our current findings provide further insights into neurobiological targets for future pharmacotherapies that attenuate unwanted negative outcomes during pain. Emerging therapies such as focused ultrasound technology (Elias et al., 2016), the development of photoactivable compounds (Banghart and Sabatini, 2012) and drugs specifically targeting the activated-KOR structure (Che et al., 2018) could allow for selective and localized treatments. Together with a better understanding of dynorphin-KOR system in pain-induced negative affect, these studies open new avenues for targeting KOR as a site for treating pain-induced emotional states.

STAR METHODS

CONTACT FOR REAGENT AND RESOURCE SHARING

Further information and requests for resources and reagents should be directed to and will be fulfilled by the Lead Contact, Jose A. Morón (jmoron-concepcion@wustl.edu).

EXPERIMENTAL MODEL AND SUBJECT DETAILS

All procedures were approved by the Washington University Institutional Animal Care and Use Committee (IACUC) in accordance with the National Institutes of Health Guidelines for the Care and Use of Laboratory Animals. Adult male Sprague Dawley rats (250-300g), adult male and females dynorphin-cre (dyn-Cre) mice (25-30g) (Al-Hasani et al., 2015), adult male and females Ai14 or Ai9 preprodynorphin reporter mice (Al-Hasani et al., 2015; Krashes et al., 2014) (25-30g) and adult C57Bl/6J males and females mice (25-30g) were used for this study. All animals were 10 to 12 weeks at the beginning of the experiments. Two to three rats were housed together with a 12/12 hours dark/light cycle (lights on at 7:00 AM) and acclimated to the animal facility holdings for at least 7 days before any manipulation. Rats received food *ad libitum* until 2 days before starting the behavioral studies, when food restriction (17 g of rat chow per day) started and continued until the end of the experiment. Four to five mice were housed together, given access to food pellets and water ad libitum, and maintained on a 12/12 h dark/light cycle (lights on at 7:00 AM). All animals were kept in a sound-attenuated, isolated holding facility in the lab 1 week prior to surgery, post-surgery, and throughout the duration of the behavioral assays to minimize stress.

METHOD DETAILS

SURGERIES—All surgeries were performed under isoflurane (1.5/2 MAC) anesthesia under sterile conditions. Intra cerebral injections:

Rats were stereotaxically (World Precision Instruments, Sarasota, FL) injected with either norBNI (2μg per side in 0.5μl), HSV-Dyn2.0-hM4di-IRES-mCherry (5×10^8 transducing units per ml - 0.5μl per side), HSV-Dyn2.0-mCherry (5×10^8 transducing units per ml - 0.5μl per side) or implanted with guide cannula (Plastics One, Roanoke, VA) targeting the

NAcShCS (stereotaxic coordinates from Bregma: A/P = + 0.96mm, M/L = ± 0.8mm, D/V = – 6.5mm from the skull surface) (Castro and Berridge, 2014; Hipólito et al., 2015). Animal's skin was either sutured after bilateral injection using sterile nylon sutures or, when using guide cannula, the implants were secured on the skull using two sterile bone screws and a dental cement head-cap (Lang Dental). Cannula were obstructed using a dummy cannula and covered by a cannula cover until pharmacological injection.

Mice were anesthetized in an induction chamber (4 MAC Isoflurane) and placed into a stereotaxic frame (Kopf Instruments, Model 1900) where they were maintained at 1 MAC–2 MAC isoflurane. A craniotomy was performed and followed by a unilaterally injection, using a blunt needle (86200, Hamilton Company), 300nl of AAV5-DIO-ChR2-eYFP or AAV5-DIO-eYFP controls (Hope Center Viral Vector Core, viral titer 2×10^{13} vg/ml) into vNAcSh (stereotaxic coordinates from Bregma: A/P: + 1.30mm, M/L: ± 0.5mm, D/V: −4.75mm) (Al-Hasani et al., 2015). Two weeks after this injection mice underwent a second surgery where norBNI (2 μg or 4 μg /0.5 μl) was locally injected and a fiber optic was placed in the vNAcSh (Al-Hasani et al., 2015; Siuda et al., 2015). The implants were secured using two bone screws and a dental cement head-cap (Lang Dental). Mice were allowed to recover one week before running any behavioral experiment, well within the limits of norBNI antagonism. Furthermore, the experiments started 3 weeks after AAV5-DIO-ChR2-eYFP injection, permitting optimal expression of ChR2 in the dyn-Cre cell bodies.

A similar surgical procedure was used for pharmacological microinjection of norBNI (Figure 1E-H). Briefly, following craniotomy norBNI (2 μg or 4 μg /0.5 μl) was bilaterally injected into vNAcSh (stereotaxic coordinates from Bregma: A/P: + 1.30mm, M/L: ± 0.5mm, D/V: −4.75mm)[5]. Mice's skin was sutured after bilateral injection using sterile nylon sutures and this animal was allowed to recovery for a week before running any behavioral experiment.

CFA administration: After confirming sedation by the absence of reflex during a toe-pinch, rats and mice were injected with in the right hindpaw with properly resuspended 150ul or 50ul of CFA solution (Thermo Fisher), respectively. Animal' recovery and general behavior (feeding, drinking, mobility) were monitored through the rest of the experiment.

CHEMOGENETICS, OPTOGENETICS AND BEHAVIORAL ASSAYS

Sucrose Self-administration: Rat operant-conditioning chambers (Med Associates, Fairfax, VT) were equipped with two retractable levers positioned on the right-hand wall 12.5 cm apart and 5 cm above the floor, a food magazine connected to a food pellet dispenser, two cue lights positioned 2 cm above the levers, and one house light positioned on the top left-hand wall. At the beginning of the session, both levers (active and inactive) were presented and a white light was on above the active lever. Pressing the active lever resulted in sucrose pellet dispense and a 20 seconds' retraction of both active and inactive levers, along with the turning off of the light cue above the active lever after the retraction of the levers. Pressing the inactive lever had no effect. Animals were gently placed in the self-administration boxes for 2 hour sessions where a press on the active lever results in sucrose pellet dispense - fixed-ratio (FR) 1 schedule. Once rats acquired the self-administration

behavior (by obtaining 60 pellets/session on 5 consecutive sessions), the schedule of reinforcement was changed to FR2 for the other 3 sessions, and then FR5 for another 3 sessions. Once they completed the training, the rat's motivation for sucrose self-administration was tested using a Progressive Ratio (PR) schedule of reinforcement (PR1). In the PR session, the number of responses on the active lever to obtain the reward increased with the dose. The increase in the number of correct responses followed the equation response ratio = $(5 \times e^{(0.2 \times \text{Infusion number})} - 5$ rounded to the nearest integer resulting in the following PR steps: 1, 2, 6, 9, 12, 15, 20, 25, 32, 40, 50, 62, 77, 95… (Hipólito et al., 2015; Roberts and Bennett, 1993; Schwartz et al., 2014)

For the studies on the necessity of KOR on pain effects on motivated behavior, rats were injected with either norBNI (2 μg per side) or aCSF in the NAcShCS (A/P: + 0.96mm; M/L: +/− 0.8mm; D/V: - 6.5mm) (Castro and Berridge, 2014). A week after, to allow full recovery, animals were tested on a second PR schedule of reinforcement (PR2) to assess any effect of KOR antagonism on motivation. Right after, rats were injected with 150 μl of saline or CFA solution in the hindpaw; and placed again in the self-administration chambers 48 hours after injection to undergo an additional PR session.

For the studies on the sufficiency of KOR on pain effects on motivated behavior, after training and a first PR ratio (PR1) as a baseline measurement, rats were deeply anesthetized and guide cannula were placed bilaterally 1mm above the NAcShCS (A/P: - 0.96mm; M/L: +/− 0.8mm; D/V: - 5.5mm) (Castro and Berridge, 2014). One week after surgery, to allow full recovery, animals were injected in the NAcShCS with KOR agonist (U50,488 – 1 μg per side) or aCSF using a microinjection pump (rate 0.25 μg per minute) and the injector, projecting 1mm below the cannula, was left in place for an additional 5 minutes to allow compound diffusion. 30 minutes after U50,488 injection rats were tested for thermal hyperalgesia using Hargreaves test. 30 minutes later these animals were gently placed in the self-administration boxes for a second PR test (PR2), thus assessing the role of KOR stimulation on sucrose self-administration. Lastly, and because U50,488 is a reversible KOR agonist, a third PR test was performed 24 hours later to assess if the effects of KOR activation were transient or sustainable.

To determine the involvement of KOR stimulation during a FR schedule of reinforcement, animals were trained to self-administer sucrose as pellets as mentioned above. After completion of three successive FR5 sessions, rats were deeply anesthetized and guide cannula were placed bilaterally 1mm above the NAcShCS (A/P: - 0.96mm; M/L: +/− 0.8mm; D/V: - 5.5mm) (Castro and Berridge, 2014). A week after surgery, to allow full recovery, animals were injected in the NAcShCS with KOR agonist (U50,488 – 1 μg per side) or aCSF using a microinjection pump (rate 0.25 μg per minute) and the injector was left in place for an additional 5 minutes to allow compound diffusion. 1 hour after U50,488 injection rats were gently placed in the self-administration boxes for new FR5 session, thus assessing the role of KOR stimulation on a fixed ratio schedule of reinforcement for sucrose self-administration.

For the studies on the necessity of dynorphin containing neurons activity on pain effects on motivated behavior rats were injected with either HSV-Dyn2.0-hM4Di-IRES-mCherry,

HSV-Dyn2.0- mCherry (0.5 µl per side, viral titer: 5×10^8 transducing units per ml, provided by Rachael Neve, MIT, Boston, Massachusetts) or aCSF in the NAcShCS (A/P: +0.96mm; M/L: +/−0.8mm; D/V: −6.5mm). Three days after, animals were injected with 150 µl of saline or CFA solution in the hindpaw; and 48 h later, when inflammation was stable, the rats were injected *i.p* with CNO (1 mg.kg-1) or saline as a control and placed again in the self-administration chambers to undergo a second PR session 15 minutes after *i.p.* treatment.

For assessment of motivation in mice a PR schedule of reinforcement for sucrose pellet self-administration was also used and performed as described above with slight modifications. Mice operant-conditioning chambers (Med Associates, Fairfax, VT) were equipped with nose poke holes, both presenting a cue light, accessible to animals. An active nose poke resulted in a sucrose delivery in the food magazine together with house light cue for 20 seconds (FR1). During this 20 seconds period, no further action had consequence (time out period). Poking in the inactive hole had no consequence. Mice were trained to discriminate in between active and inactive lever during one hour long FR1 sessions. Once discrimination was acquired (less than 30% of total poking in the inactive hole), mice underwent 3 consecutive sessions of FR2 and 3 consecutive sessions of FR5. Mice's motivation was then assessed using a 1 hour session of progressive ratio schedule of reinforcement. To test the necessity of KOR to drive pain-induced negative affect, intra accumbal (AP: +1.3mm; L: +/− 0.5mm; DV: −4.75mm) injection of 0.5 µl of either aCSF or norBNI (2µg per side) were then performed. After surgery recovery, a second progressive ratio testing was performed to assess the consequences of kappa opioid receptors antagonism on mice's motivation (PR2). Following this, 50nl of either sterile saline or CFA solution was injected the mice' right hindpaw. 48 hours later, when inflammation is stable, animals underwent a third progressive ratio session. To test the sufficiency of dynorphin-containing neurons photostimulation to drive negative affective states, dynorphin-Cre mice received an injection of AAV cre-dependent channelrhodopsin in the vNAcSh (AP: +1.3mm; L: +/− 0.5mm; DV: −4.75mm). After two weeks recovery, using the same stereotaxic coordinates, the animals were implanted with fiber implant in the vNAcSh. Training period was then performed as described above a week after surgery to allow full recovery. Following training the animals were exposed to a PR session in which fiber implant was connected to a 473nm laser emitting constant photo-stimulation (20Hz, 10msec width) during the test.

Plantar test for thermal sensitivity – Hargreaves test: The hyperalgesic effects induced by CFA injection in the rat's hindpaw were examined using the thermal plantar test (Hargreaves method, IITC Life Science). Animals were placed in Plexiglas boxes on top of a glass surface. After 30 min of habituation, a radiant heat source was applied on the plantar surface of the right hindpaw, and the latency of paw withdrawal from the radiant heat stimulus was recorded. Four measurements with at least a 5-min interval between trials were obtained for each session. The intensity of the light beam was adjusted so that baseline latencies were 15 s in naive rats. A cutoff time of 30 s was imposed to prevent tissue damage. Paw withdrawal thresholds (4 measurements with 5 min of resting period) were measured for 5 consecutive days during the four last sucrose self-administration training

days. These thermal sensitivity recordings were repeated 30 minutes before any progressive ratio schedule of reinforcement test to confirm inflammation-induced hyperalgesia.

Real Time Place Testing (RTPT): All behaviors were performed within a sound-attenuated room maintained at 23°C at least 1 week after habituation to the holding room and the final surgery. Lighting was stabilized at ~1,500 lux for aversion behaviors, ~250 lux for anxiety-like behaviors. Movements were video recorded and analyzed using Ethovision XT 10.0 (Noldus Information Technologies).

For real time place testing, after recovery from surgery (please refer to the surgeries section for further information on procedure) mice were gently placed in a custom-made unbiased, balanced two-compartment conditioning apparatus (52.5 × 25.5 × 25.5 cm) as described previously (Al-Hasani et al., 2015; McCall et al., 2015; Siuda et al., 2015). During a 20-min trial, entry into one compartment triggered photo-stimulation (20Hz, 10ms pulse width) while the animal remained in the light-paired chamber and entry into the other chamber ended photo-stimulation.

Open Field Test: Open field testing was performed in a square enclosure (55 × 55 cm) within a sound attenuated room maintained at 23°C. Lighting was measured and stabilized at ~25 lux. Mice were placed in the center of the open field and allowed to roam freely for 21 min. Throughout the 21 minutes mice received constant photo-stimulation (20Hz, 10ms pulse width). The open field was cleaned with 70% ethanol between each trial. Movements were video recorded and analyzed using Ethovision XT 10.0 (Noldus Information Technologies, Leesburg, VA). The center was defined as a square comprised of 50% the total area of the open field chamber. Time in the center was the primary measure of anxiety-like behaviors.

RECEPTOR FUNCTION ASSESSMENT

Incorporation of GTPγS in membranes: NAc tissue was micro-dissected from saline and CFA-injected rat and tested in GTPγS coupling assay as described previously (Kissler et al., 2014), with slight modifications. Briefly, tissue was homogenized (40-45 strokes; glass homogenizer with Teflon plunger; on ice) in 1.5 ml of membrane buffer (pH 7.4, 50.0 mM Tris–HCl, 3.0 mM MgCl2, and 1.0 mM EGTA). Homogenates were centrifuged (15000rpm, 4°C for 30 min), re-suspended in 1.5 ml membrane buffer, homogenized (12-15 strokes; on ice) again and finally centrifuged. Pellet was homogenized (12-15 strokes; on ice) in 1.5 ml assay buffer (pH 7.4, 50.0 mM Tris–HCl, 3.0 mM MgCl2, 0.2 mM EGTA, 100.0 mM NaCl). Protein estimation was conducted using BCA protein assay (Pierce). Protein (5.0 μg) was homogenized (12-15 strokes; on ice) and incubated with Dynorphin A (0.1-1.0 uM), at least in duplicate, in assay buffer for 90 min at 25°C, with 10 μM GDP and 0.4 nM [^{35}S] GTPγS in a total volume of 250.0 μl. Unlabeled GTPγS (10.0 μM) was used to assess nonspecific binding. Specific binding was obtained by subtracting nonspecific binding from total binding. The reaction was quickly terminated by filtration through UniFilter-96 GF/B filter plates using a cell harvester (Brandel, Gaithersburg, MD), followed by 8-10 washes with wash buffer (ice-cold phosphate buffer (pH 7.4), 5.0 mM MgCl2). Bound radioactivity on the filters was counted by Microbeta liquid scintillation counter (PerkinElmer Life Sciences)

on the following day. GTPyS coupling data was analyzed using a mixed-model two-way ANOVA to compare changes in GTPγS signaling for the controls and CFA-treated animals. The within-subject variable was DYN concentration and the between-groups variable was treatment condition.

Incorporation of GTPγS in slices (autoradiography): Brains were collected from saline or CFA injected rats 48h post-injection and were snap-frozen with isopentane at −30 °C, and stored in −80 °C until fu rther processing. The brains were then coronal-sectioned via cryostat (20 μm thick) at −20 °C, and thaw-mounted on SuperFrost charged slides. Sections were pre-incubated in assay buffer (50mM Tris-HCl, 3mM MgCl2, 0.2mM EGTA, 100 mM NaCl, 2 mM GDP, 1 μM DPCPX, pH=7.4) for 15 min. Agonist-stimulated KOR activity was determined by incubating brain sections in [^{35}S] GTPγS (40 pM) with U69,593 (10 μM) +/− JdTic (10 μM) for 1 hour at RT. After incubation, slides were washed 2x in ice-cold wash buffer (50 mm Tris-HCl, pH 7.4) followed by a brief wash in ice-cold deionized water (30 sec). Slides were air-dried and exposed to Kodak Biomax film together with [^{14}C] standards for 2 days. Films were developed using Kodak GBX Developer and RapidFix solutions. Films were digitally analyzed and quantified using MicroComputer Image Device (MCID) normalized to the [^{14}C] standard curve, measured in dpm/mg (MCID Imaging Research, St. Catherine, Ontario, Canada). The resulting agonist-stimulated samples were compared to non-agonist-treated brain samples to determine the percent activation of KOR above basal.

Slices radiography for KOR occupancy: Brains were dissected and frozen for cryostat sectioning. Coronal, 50μm thick sections were thaw-mounted in pairs on poly-L-lysine microscope slides and allowed to air-dry. The slides were then stored at −80 until used. Slides were removed from the −80 and allowed to warm to room temperature. Paired sections were traced around using a hydrophobic pen. Each paired section was filled with 1.0ml of either 50μci/ml of [^{11}C]-LY2795050 and allowed to incubate for the allotted time (10-40 mins). Once the incubation time is complete, the radiopharmaceutical was removed and MilliQ water was replaced in the barrier area for approximately 10 second. The MilliQ wash was repeated 3 times. Slides were allowed to air dry. The slides were then placed in a cassette and exposed to the phosphor imaging screen overnight. The screen was then imaged using the typhoon imager.

ELECTROPHYSIOLOGY

In vitro electrophysiological experiments on brain slices were conducted 48 hours after saline or CFA injection in the hindpaw.

To measure dynorphin neurons excitability, male and female Ai14-Dynorphin-Cre mice (5-10 weeks old) were deeply anesthetized with isoflurane and perfused transcardially with 34°C aCSF (in mM as follows: 0.001 MK-801, 126 NaCl, 2.5 KCl, 1.4 NaH2PO4, 1.2 MgCl2, 2.4CaCl2, 11 glucose, and 25 NaHCO3) before being decapitated. Brains were quickly removed and submerged in warm MK-801-buffered aCSF. Coronal forebrain sections (230–250 μm) that contained the NAc were cut using a vibratome (VT1200S, Leica Microsystems) in warm aCSF containing 1 μM MK-801. NAc slices were submerged in

aCSF (in mM as follows: 0.01 MK-801 126 NaCl, 2.5 KCl, 1.4 NaH2PO4, 1.2 MgCl2, 2.4CaCl2, 11 glucose, and 25 NaHCO3) at 34°C for 30 m, and equilibrated with 95% O2 and 5% CO2 before maintenance at room temperature in aCSF without MK-801. Slices were then individually transferred to the recording chamber (volume 0.8 ml) and superfused continuously (2.2 ml/min) with 34°C aCSF. NAc neurons were visualized using differential interference contrast optics on an upright microscope (BX50WI, Olympus). Ai14 reporter animals contain a cre-dependent tdTomato, which was visualized using a 530 nM light shone through the 40X objective. Whole-cell current-clamp recordings of NAc neurons were obtained using an Axopatch 200B amplifier (Molecular Devices). Electrodes (3–4.5 MΩ) were filled with pipette solution containing the following (in mM): 120 K-gluconate, 5 NaCl, 2 $MgCl^2$, 0.1 $CaCl^2$, 10 HEPES, 1.1 EGTA, 4 Na^2ATP, 0.4 Na^2GTP, 10 Na^2Phosphocreatine, and 0.05% biocytin. The internal solution had pH 7.3 and osmolality 288 mOsm/l. Membrane voltage and cellular responses to current steps (−50 pA, Δ5 pA, 200ms) were recorded in the presence of DNQX (5 μM), strychnine (5 μM), CGP 55845 (1 μM), and APV (50 μM). All recordings were filtered (2 kHz low-pass filter) and sampled (10 kHz) for online and later offline analysis (Axograph X; Axograph Scientific Software).

To assess sIPSCs, whole-cell voltage clamp experiments on brain slices were conducted 48 hours after saline or CFA injection in the hindpaw. Male and female Ai9-Dynorphin-Cre mice (8-10 weeks old) were deeply anesthetized with a cocktail of ketamine/xylazine/acepromazine and perfused transcardially with NMDG-substituted aCSF containing (in mM): 93 NMDG, 2.5 KCl, 1.25 NaH2PO4, 30 NaHCO3, 20 HEPES, 25 glucose, 5 ascorbic acid, 2 thiourea, 3 Na-pyruvate, 12 N-acetyl-L-cysteine, 10 MgSO4, 0.5 CaCl2, pH=7.3. After decapitation, 300 μm thick coronal sections containing the NAc were cut using a Vibratome VT1000s (Leica) and transferred to an oxygenated recovery chamber containing NMDG aCSF for 10–12 minutes at 32–34°C, before being transferred to a holding chamber filled with aCSF containing (in mM): oxygenated aCSF containing (in mM): 124 NaCl, 2.5 KCl, 1.25 NaH2PO4, 24 NaHCO3, 5 HEPES, 12.5 glucose, 2 CaCl2, 1 MgCl2; pH=7.3, 300-315 mOsm and were incubated in the dark at room temperature for >1 hr before recording. Slices were transferred to a heated (32-34°C) recording chamber in the dark and perfused (~2 mL/min) with oxygenated aCSF containing. Dynorphinergic neurons in the NAc were visualized through a 40x objective using IR-DIC microscopy on an Olympus BX51 microscope, and tdT+ neurons were identified using epifluorescent illumination. Electrodes (3–4.5 MΩ) were filled with pipette solution containing the following (in mM): 110 D-gluconic acid, 110 CsOH, 0.1 CaCL2, 4 MG2ATP, 0.4 Na2GTP, 10 Na2Phosphocreatine, 10 HEPES, 1.1 EGTA, 8 TEA+CL−, 3 QX314+Br−, and 0.05% neurobiotin. The internal solution had pH 7.3 and osmolality 290 mOsm/l. Recordings were made with Patchmaster software controlling a HEKA EPC10 and EPC10 Double amplifiers. Following gigaseal formation and stable whole-cell access, spontaneous inhibitory postsynaptic currents were isolated by blocking AMPA/KARs (10 μM NBQX, Abcam) and NMDARs (50 μM D-APV, Abcam). Neurons were voltage clamped at 0 mV and whole-cell currents were recorded using a gap-free protocol. In a subset of cells, $GABA_A$Rs were then blocked using 100 μM picrotoxin (Abcam) and 10 μM biccuculine to confirm as $GABA_A$R IPSCs. Only cells with a stable Rs (+/− 20%) less than 15 MOhm were included in our

analysis. For sIPSC recordings, amplitude, frequency, and the kinetics of currents were extracted offline using the Mini Analysis software (Synaptosoft).

Ex vivo confirmation of Gi-DREADD functionality was performed using whole cell-patch clamp electrophysiology (recording details below). Rats were injected with either HSV-Dyn2.0-hM4Di-IRES-mCherry or HSV-Dyn2.0- mCherry in the NAcShCS. Three to five days later, animals were sacrificed and brains were extracted for current-clamp recordings of NAc neurons. Membrane voltage and cellular responses to current steps were recorded in the presence of DNQX (5 μm), strychnine (5 μm), CGP 55845 (1 μm), and APV (50 μm) before and during the bath application of 10 μM CNO. After the determination of baseline rheobase, current steps of 1, 2, 3 or 4 times the rheobase were applied to examine the magnitude of neuronal inhibition by CNO.

IMMUNOHISTOCHEMISTRY

Dynorphin HRP staining: Rats were pretreated with 20 μg colchicine (Sigma-Aldrich) through *i.c.v.* injection (stereotaxic coordinates: A/P: – 1.5 mm; M/L: −0.8 mm; D/V: −4.5 mm) under isoflurane (1.5-2% MAC) anesthesia. Animals were injected with saline or CFA into the plantar surface of the hindpaw as previously described. 48 hours after, rats were trans-cardially perfused with phosphate buffered saline (PBS) followed by 4% paraformaldehyde (PFA) diluted in PBS. Brains were removed and post-fixed 20h in 4% PFA, then transferred in 30% sucrose in PBS. After flash freezing, brains were cut in 40 μm coronal slices using a cryostat (Leica CM 1950). Free-floating sections were then washed in Tris-based saline buffer (TBS) before and after every incubation. First, slices were incubated for 30 min with 1% hydrogen peroxide in TBS to quench peroxidase activity. Then they were incubated with rabbit-anti-dynorphin A (1:1000, T-4268, Peninsula Laboratories International Inc.) followed by biotinylated anti-Rabbit antibody (1:1000, BioRad) diluted in TBS - 0.3% Triton X-100 - 5% normal goat serum. Biotinylated anti-rabbit antibodies were revealed using avidin-streptavidin complex (ABC-Kit, Vector) followed by the reaction with DAB (Sigmafast, Sigma). Slices were then mounted and coversliped with Eukitt (Microptic). All pictures were taken at 10x with a Leica DMR microscope using constant set up and lighting within the same day. Image J software was used to measure I.O.D. Pictures were first converted into 8-bit (grayscale) and the background (measured as staining in the anterior commissure) was subtracted. A ROI was selected based on kappa NAcShCS[6] to measure I.O.D. in the inverted picture.

HSV/dynorphin A co-staining: Rats were injected with 20 μg colchicine (Sigma-Aldrich) through i.c.v. injection (stereotaxic coordinates: A/P: – 1.5 mm; M/L: −0.8 mm; D/V: −4.5 mm) and HSV-dyn2.0-hM4Di-IRES-mCherry in the NAc (stereotaxic coordinates from Bregma: A/P = + 0.96mm, M/L = ± 0.8mm, D/V = – 6.5mm from the skull surface) under isoflurane (1.5-2% MAC) anesthesia. Animals were transcardially perfused 24hours after injections with phosphate buffered saline (PBS) followed by 4% paraformaldehyde (PFA) diluted in PBS. Brains were removed and post-fixed 20h in 4% PFA, then transferred in 30% sucrose in PBS. After flash freezing, brains were cut in 40 μm coronal slices using a cryostat (Leica CM 1950). Free-floating sections were then washed in phosphate based saline buffer (PBS) before and after every incubation. First, slices were incubated

endogenous biotin blocking kit (ThermoFisher Scientific, USA). After PBS washes, slices were bathed with blocking solution composed of normal goat serum (5%) and 0.01% Tween 20 diluted in PBS, before being incubated with both rabbit anti-DynorphinA (1/1000, Peninsula Labs, CA) and mouse anti-mCherry (1/1000, DHBS, IO) antibodies diluted in blocking buffer overnight at 4C. Slices were then exposed to a goat anti-mouse Alexa 568 (1/500, ThermoFischer) and biotin conjugated anti-rabbit (1/500, ThermoFischer Scientific) for 2 hours at room temperature. Lastly, slices were incubated with Alexa 488 conjugated streptavidin (10μg per ml, ThermoFischer Scientific) for 2 hours at room temperature to amplify dynorphin A signal. Slices were mounted and cover slipped with HardSet DAPI staining and analyzed using a Leica confocal microscope.

POSITRON EMISSION TOMOGRAPHY (PET) IMAGING

Animals were transported to the preclinical PET imaging facility one hour before starting the experiment to allow room habituation. Preclinical PET imaging was performed on either the Siemens Inveon PET/CT or the microPET Focus F220. A 30min dynamic PET image acquisition followed a bolus injection of [^{11}C]-LY2795050 (~1mCi) via the tail-vain. [^{11}C]-LY2795050 is an antagonist of the kappa opioid receptor (KOR) and has demonstrated invaluable utility in quantifying the density and occupancy of kappa opioid receptors in numerous applications (Shoghi and Welch, 2007; Zheng et al., 2013). All PET images were reconstructed using the OSEM algorithm. Regions of interest (ROIs) were drawn on the whole brain. In the absence of a reference region in the brain, we used muscle as a reference regions to quantify the distribution volume. To calculate the distribution volume (DV), we performed Logan graphical analysis[41] using whole-brain kinetics of [^{11}C]-LY2795050 with muscle kinetics as a reference regions. The linear segment of the linearized plot of the Logan plot (Logan, 2000) was used to derive the distribution volume of the tracer as a measure of apparent receptor density/availability.

IN SITU HIBRIDIZATION

Following rapid decapitation of C57/BL6 mice, brains were rapidly frozen in 100 ml −50°C isopentane and stored at −80°C. Coronal sections containing the VTA and NAc were cut at 20 μM at −20°C and thaw-mounted onto Super Frost Plus slides (Fisher, Waltham, MA). Slides were stored at −80°C until further processing. Fluorescent in situ hybridization was performed according to the *RNAScope 2.0 Fluorescent Multiple Kit User Manual for Fresh Frozen Tissue* (Advanced Cell Diagnostics, Inc.) as described previously (Wang et al., 2012). Briefly, sections were fixed in 4% PFA, dehydrated, and treated with *pretreatment 4* protease solution. Sections were then incubated for target probes for mouse Oprk1 (Tejeda et al., 2017). Probe consisted of 20 ZZ oligonucleotides and was obtained from Advanced Cell Diagnostics. Following probe hybridization, sections underwent a series of probe signal amplification steps followed by incubation of fluorescently labeled probes designed to target the specified channel associated with Oprk1. Slides were counterstained with DAPI, and coverslips were mounted with Vectashield Hard Set mounting medium (Vector Laboratories). Images were obtained on a Leica TCS SPE confocal microscope and analyzed with Application Suite Advanced Fluorescence (Leica).

HISTOLOGY

Please refer to Figure S4. After perfusion brain were kept in 4% paraformaldehyde at 4°C for 24 hours. They were then transferred in 30% sucrose solution for two to five days (until they sank in the vial) at 4C degrees. Brain were frozen in isopentane (−80°C) for 1minute and kept in −20°C freezer until sliced using cryostat. Tissue was 40μm thick and mounted on slides. An experimenter blinded to treatments assessed guide-cannulae, fiber optic and injections placement. Only animals confirmed to have correct cannula placement were included in the final data and statistical analyses.

QUANTIFICATION AND STATISTICAL ANALYSIS

All experiments were performed at least twice, including all treatment groups in each round, to avoid any unspecific day/condition effect. Treatments (i.e. intra-NAc, inflammation and sub-cutaneous) were randomly assigned to animals before testing. Statistical significance was taken as $*p < 0.05$, $**p < 0.01$, $***p < 0.001$, and $****p < 0.0001$, as determined by a one-way ANOVA or a two-way repeated-measures ANOVA followed by a Sidak post hoc tests, two-tailed unpaired or paired t-test, one sample t-test compared to hypothetical value (50%) or Mann-Whitney for unpaired values as appropriate. All data samples were tested for normality of distribution using Shapiro-Wilk test before being assigned to ANOVAs, or t-test analysis. All data are expressed as mean ± SEM. Sample size (n number) always refers to the value obtained from an individual animal when referring to behavioral experiments (Figures 1A-L, Figure 2A-H, Figure 4A-E and Figure S1A-I) and anatomical slice analysis (Figure 3A-F, and Figure S2A-B), the total number of mCherry positive neurons (Figure S3B) or an individual cell recording (Figure 3J-P and Figure S2C-J). For experiments that include samples from model organisms, the sample size (n value) was reported as $n_{cells/animals}$ (see Figure 2G-P and Figure S3). For each experiment detailed statistical analysis and sample size (n number) are carefully reported in figure legends. Statistical analyses were performed in GraphPad Prism 6.0 and SPSS.

DATA AND SOFTWARE AVAILABILITY

Authors can confirm that all relevant data are included in the paper and its supplementary information files.

Supplementary Material

Refer to Web version on PubMed Central for supplementary material.

ACKNOWLEDGMENTS

We would like to thank all members from the Moron-Concepcion', Bruchas' and Al-Hasani' laboratories for their help throughout the completion of the current study and Lindsay Lueptow for the complementary analysis of GTPgammaS slices. This work was supported by US National Institutes of Health (NIH) grant DA041781 (J.A.M.), DA042581 (J.A.M.), DA042499 (J.A.M.), DA041883 (J.A.M.), DA045463 (J.A.M.), NARSAD Independent Investigator Award from the Brain and Behavior Research Foundation (J.A.M.), DA033396 (M.R.B), DA037152 (M.R.B.), R01-NS106953 (R.W.G.), AA020394 (B.M.W.), K99/R00-DA038725 (R.A.), K99-DA041467 (A.W-P), Philippe Foundation (N.M.), the "Spanish Ministerio de Economia y Competitividad" MINECO PSI2016-77895-R (L.H), the Mallinckrodt Institute of Radiology at Washington University from pilot grant 16-014 to support the positron emission tomography studies, the Hope Center Viral Vectors Core at Washington University School of Medicine.

REFERENCES

Al-Hasani R, McCall JG, Shin G, Gomez AM, Schmitz GP, Bernardi JM, Pyo C-O, Park SI, Marcinkiewcz CM, Crowley NA, et al. (2015). Distinct Subpopulations of Nucleus Accumbens Dynorphin Neurons Drive Aversion and Reward. Neuron 87, 1063–1077. [PubMed: 26335648]

Apkarian AV, Sosa Y, Krauss BR, Thomas PS, Fredrickson BE, Levy RE, Harden RN, and Chialvo DR (2004). Chronic pain patients are impaired on an emotional decision-making task. Pain 108, 129–136. [PubMed: 15109516]

Baldo BA, Daniel RA, Berridge CW, and Kelley AE (2003). Overlapping distributions of orexin/hypocretin- and dopamine-beta-hydroxylase immunoreactive fibers in rat brain regions mediating arousal, motivation, and stress. J. Comp. Neurol 464, 220–237. [PubMed: 12898614]

Banghart MR, and Sabatini BL (2012). Photoactivatable neuropeptides for spatiotemporally precise delivery of opioids in neural tissue. Neuron 73, 249–259. [PubMed: 22284180]

Borsook D, Becerra L, Carlezon WA, Shaw M, Renshaw P, Elman I, and Levine J (2007). Reward-aversion circuitry in analgesia and pain: implications for psychiatric disorders. Eur. J. Pain Lond. Engl 11, 7–20.

Bruchas MR, Land BB, Lemos JC, and Chavkin C (2009). CRF1-R activation of the dynorphin/kappa opioid system in the mouse basolateral amygdala mediates anxiety-like behavior. PloS One 4, e8528. [PubMed: 20052275]

Bruchas MR, Land BB, and Chavkin C (2010). The dynorphin/kappa opioid system as a modulator of stress-induced and pro-addictive behaviors. Brain Res. 1314, 44–55. [PubMed: 19716811]

Castro DC, and Berridge KC (2014). Opioid hedonic hotspot in nucleus accumbens shell: mu, delta, and kappa maps for enhancement of sweetness “liking” and “wanting.” J. Neurosci. Off. J. Soc. Neurosci 34, 4239–4250.

Chavkin C (2011). The therapeutic potential of κ-opioids for treatment of pain and addiction. Neuropsychopharmacol. Off. Publ. Am. Coll. Neuropsychopharmacol 36, 369–370.

Chavkin C, and Martinez D (2015). Kappa Antagonist JDTic in Phase 1 Clinical Trial. Neuropsychopharmacology 40, 2057–2058. [PubMed: 26174493]

Che T, Majumdar S, Zaidi SA, Ondachi P, McCorvy JD, Wang S, Mosier PD, Uprety R, Vardy E, Krumm BE, et al. (2018). Structure of the Nanobody-Stabilized Active State of the Kappa Opioid Receptor. Cell 172, 55–67.e15. [PubMed: 29307491]

Crowley NA, and Kash TL (2015). Kappa Opioid Receptor Signaling In the Brain: Circuitry and Implications for Treatment. Prog. Neuropsychopharmacol. Biol. Psychiatry 62, 51–60. [PubMed: 25592680]

Crowley NA, Bloodgood DW, Hardaway JA, Kendra AM, McCall JG, Al-Hasani R, McCall NM, Yu W, Schools ZL, Krashes MJ, et al. (2016). Dynorphin Controls the Gain of an Amygdalar Anxiety Circuit. Cell Rep. 14, 2774–2783. [PubMed: 26997280]

Elias WJ, Lipsman N, Ondo WG, Ghanouni P, Kim YG, Lee W, Schwartz M, Hynynen K, Lozano AM, Shah BB, et al. (2016). A Randomized Trial of Focused ultrasound Thalamotomy for Essential Tremor. N. Engl. J. Med 375, 730–739. [PubMed: 27557301]

Elman I, and Borsook D (2016). Common Brain Mechanisms of Chronic Pain and Addiction. Neuron 89, 11–36. [PubMed: 26748087]

Elman I, Borsook D, and Volkow ND (2013). Pain and suicidality: insights from reward and addiction neuroscience. Prog. Neurobiol. 109, 1–27. [PubMed: 23827972]

Hipólito L, Wilson-Poe A, Campos-Jurado Y, Zhong E, Gonzalez-Romero J, Virag L, Whittington R, Comer SD, Carlton SM, Walker BM, et al. (2015). Inflammatory Pain Promotes Increased Opioid Self-Administration: Role of Dysregulated Ventral Tegmental Area μ Opioid Receptors. J. Neurosci. Off. J. Soc. Neurosci 35, 12217–12231.

Kissler JL, Sirohi S, Reis DJ, Jansen HT, Quock RM, Smith DG, and Walker BM (2014). The One-Two Punch of Alcoholism: Role of Central Amygdala Dynorphins/Kappa-Opioid Receptors. Biol. Psychiatry 75, 774–782. [PubMed: 23611261]

Knoll AT, and Carlezon WA (2010). Dynorphin, stress, and depression. Brain Res. 1314, 56–73. [PubMed: 19782055]

Krashes MJ, Shah BP, Madara JC, Olson DP, Strochlic DE, Garfield AS, Vong L, Pei H, Watabe-Uchida M, Uchida N, et al. (2014). An excitatory paraventricular nucleus to AgRP neuron circuit that drives hunger. Nature 507, 238–242. [PubMed: 24487620]

Land BB, Bruchas MR, Lemos JC, Xu M, Melief EJ, and Chavkin C (2008). The dysphoric component of stress is encoded by activation of the dynorphin kappa-opioid system. J. Neurosci. Off. J. Soc. Neurosci 28, 407–414.

Land BB, Bruchas MR, Schattauer S, Giardino WJ, Aita M, Messinger D, Hnasko TS, Palmiter RD, and Chavkin C (2009). Activation of the kappa opioid receptor in the dorsal raphe nucleus mediates the aversive effects of stress and reinstates drug seeking. Proc. Natl. Acad. Sci. U. S. A 106, 19168–19173. [PubMed: 19864633]

Leitl MD, Onvani S, Bowers MS, Cheng K, Rice KC, Carlezon WA, Banks ML, and Negus SS (2014). Pain-related depression of the mesolimbic dopamine system in rats: expression, blockade by analgesics, and role of endogenous κ-opioids. Neuropsychopharmacol. Off. Publ. Am. Coll. Neuropsychopharmacol 39, 614–624.

Liu S, Cook C, Thai E, Pickens S, Taylor AM, Tea VD, Carroll FI, Leslie FM, Evans CJ, and Cahill CM (2016). Neuropathic Pain Alters Reward and Affect via Kappa Opioid Receptor (KOR) Upregulation. FASEB J. 30, 928.5–928.5.

Logan J (2000). Graphical analysis of PET data applied to reversible and irreversible tracers. Nucl. Med. Biol 27, 661–670. [PubMed: 11091109]

Margolis EB, Hjelmstad GO, Bonci A, and Fields HL (2003). Kappa-opioid agonists directly inhibit midbrain dopaminergic neurons. J. Neurosci. Off. J. Soc. Neurosci 23, 9981–9986.

McCall JG, Al-Hasani R, Siuda ER, Hong DY, Norris AJ, Ford CP, and Bruchas MR (2015). CRH engagement of the locus coeruleus noradrenergic system mediates stress-induced anxiety. Neuron 87, 605–620. [PubMed: 26212712]

Muschamp JW, and Carlezon WA (2013). Roles of nucleus accumbens CREB and dynorphin in dysregulation of motivation. Cold Spring Harb. Perspect. Med 3, a012005. [PubMed: 23293139]

Narita M, Kishimoto Y, Ise Y, Yajima Y, Misawa K, and Suzuki T (2005). Direct evidence for the involvement of the mesolimbic kappa-opioid system in the morphine-induced rewarding effect under an inflammatory pain-like state. Neuropsychopharmacol. Off. Publ. Am. Coll. Neuropsychopharmacol 30, 111–118.

Nestler EJ, and Carlezon WA (2006). The mesolimbic dopamine reward circuit in depression. Biol. Psychiatry 59, 1151–1159. [PubMed: 16566899]

Okun A, McKinzie DL, Witkin JM, Remeniuk B, Husein O, Gleason SD, Oyarzo J, Navratilova E, McElroy B, Cowen S, et al. (2016). Hedonic and motivational responses to food reward are unchanged in rats with neuropathic pain. Pain 157, 2731–2738. [PubMed: 27548047]

Peyron C, Tighe DK, van den Pol AN, de Lecea L, Heller HC, Sutcliffe JG, and Kilduff TS (1998). Neurons containing hypocretin (orexin) project to multiple neuronal systems. J. Neurosci. Off. J. Soc. Neurosci 18, 9996–10015.

Ren W, Centeno MV, Berger S, Wu Y, Na X, Liu X, Kondapalli J, Apkarian AV, Martina M, and Surmeier DJ (2016). The indirect pathway of the nucleus accumbens shell amplifies neuropathic pain. Nat. Neurosci 19, 220–222. [PubMed: 26691834]

Roberts DC, and Bennett SA (1993). Heroin self-administration in rats under a progressive ratio schedule of reinforcement. Psychopharmacology (Berl.) 111, 215–218. [PubMed: 7870955]

Roth BL (2016). DREADDs for Neuroscientists. Neuron 89, 683–694. [PubMed: 26889809]

Schwartz N, Temkin P, Jurado S, Lim BK, Heifets BD, Polepalli JS, and Malenka RC (2014). Chronic pain. Decreased motivation during chronic pain requires long-term depression in the nucleus accumbens. Science 345, 535–542. [PubMed: 25082697]

Shippenberg TS, Stein C, Huber A, Millan MJ, and Herz A (1988). Motivational effects of opioids in an animal model of prolonged inflammatory pain: alteration in the effects of kappa- but not of mu-receptor agonists. Pain 35, 179–186. [PubMed: 2853321]

Shoghi KI, and Welch MJ (2007). Hybrid image and blood sampling input function for quantification of small animal dynamic PET data. Nucl. Med. Biol 34, 989–994. [PubMed: 17998103]

Siuda ER, Copits BA, Schmidt MJ, Baird MA, Al-Hasani R, Planer WJ, Funderburk SC, McCall JG, Gereau RW, and Bruchas MR (2015). Spatiotemporal Control of Opioid Signaling and Behavior. Neuron 86, 923–935. [PubMed: 25937173]

Tejeda HA, Wu J, Kornspun AR, Pignatelli M, Kashtelyan V, Krashes MJ, Lowell BB, Carlezon WA, and Bonci A (2017). Pathway- and Cell-Specific Kappa-Opioid Receptor Modulation of Excitation-Inhibition Balance Differentially Gates D1 and D2 Accumbens Neuron Activity. Neuron 93, 147–163. [PubMed: 28056342]

Verdejo-García A, López-Torrecillas F, Calandre EP, Delgado-Rodríguez A, and Bechara A (2009). Executive function and decision-making in women with fibromyalgia. Arch. Clin. Neuropsychol. Off. J. Natl. Acad. Neuropsychol 24, 113–122.

Wang F, Flanagan J, Su N, Wang L-C, Bui S, Nielson A, Wu X, Vo H-T, Ma X-J, and Luo Y (2012). RNAscope: a novel in situ RNA analysis platform for formalin-fixed, paraffin-embedded tissues. J. Mol. Diagn. JMD 14, 22–29. [PubMed: 22166544]

Yang H, de Jong JW, Tak Y, Peck J, Bateup HS, and Lammel S (2018). Nucleus Accumbens Subnuclei Regulate Motivated Behavior via Direct Inhibition and Disinhibition of VTA Dopamine Subpopulations. Neuron 97, 434–449.e4. [PubMed: 29307710]

Zheng M-Q, Nabulsi N, Kim SJ, Tomasi G, Lin S, Mitch C, Quimby S, Barth V, Rash K, Masters J, et al. (2013). Synthesis and Evaluation of 11C-LY2795050 as a κ-Opioid Receptor Antagonist Radiotracer for PET Imaging. J. Nucl. Med 54, 455–463. [PubMed: 23353688]

HIGHLIGHTS

- Pain recruits the dynorphin/kappa opioid receptor system in the nucleus accumbens
- Inhibitory inputs onto dynorphin cells are reduced during inflammatory pain
- Increase in dynorphin tone mediates inflammatory pain-induced negative affect

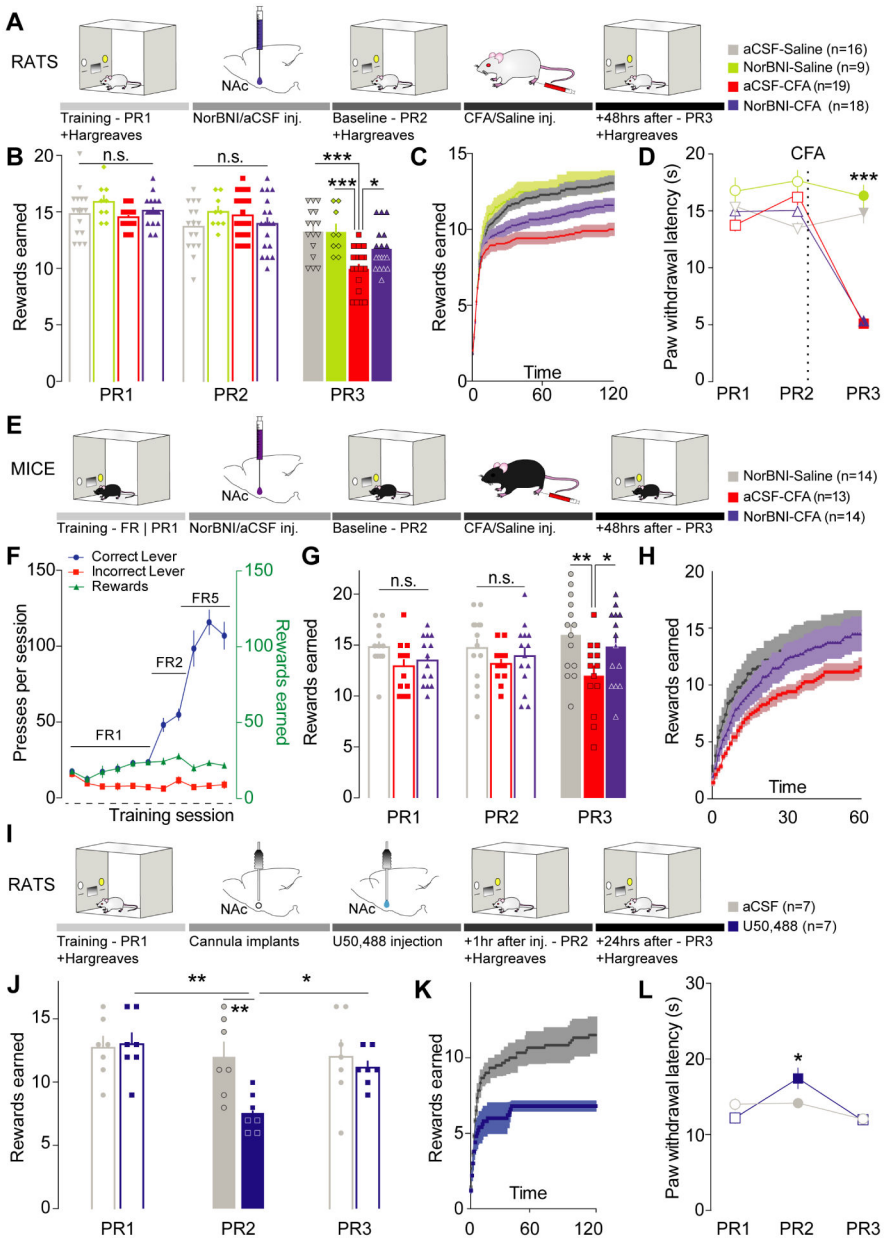

Figure 1: Kappa opioid receptors are both necessary and sufficient to drive pain-induced negative affect.

(A) Schematic representation of the behavioral methodology. (B) Blockade of KORs in the NAcShCS prevented pain-induced decrease in motivation (two-way ANOVA for repeated measures: time: $F_{2,116}$=69.51, p<0.0001; interaction: $F_{6,116}$= 7.349, p<0.0001. Post-hoc during PR3: aCSF-Saline (n=16) vs. aCSF-CFA (n=19), p<0.0001, norBNI-Saline (n=9) vs. aCSF-CFA (n=19), p<0.0001 and aCSF-CFA (n=19) vs. norBNI-CFA (n=18), p=0.0225). (C) Representation of the average number of rewards obtained every minute across the 2-hour PR3 test session. (D) Paw withdrawal latency was unchanged in inflamed animals treated with norBNI (two-way ANOVA for repeated measures: time: $F_{2,116}$=35.95, p<0.0001; treatment: $F_{3,58}$= 25.08, p<0.0001; interaction: $F_{6,116}$= 74.93, p<0.0001. Post-

hoc during PR3: aCSF-CFA (n=19) vs. norBNI-CFA (n=18), p=0.9998). (E) Schematic representation of the behavioral methodology. (F) Representation of training process across experimental days. (G) Blockade of KORs in the vNAcSh prevented the pain-induced decrease in motivation (two-way ANOVA for repeated measures: time: $F_{2,76}$= 0.5201, p<0.0001; treatment: $F_{2, 38}$= 3.432, p=0.0426. Post-hoc: norBNI-Saline (n=14) vs. aCSF-CFA (n=13), p=0.0023 and aCSF-CFA (n=13) vs. norBNI-CFA (n=14), p=0.0408). (H) Representation of the average number of rewards obtained every minute across the PR3 session. (I) Schematic representation of the behavioral methodology. (J) Stimulation of KORs in the NAcShCS by U50,488 injection is sufficient to decrease motivation (two-way ANOVA for repeated measures: time: $F_{2, 24}$=4.767, p=0.0181; treatment: $F_{1, 12}$=6.005, p=0.0306. Post-hoc after treatment (PR2): aCSF (n=7) vs. U50,488 (n=7), p=0.0064 and 24h after injection: p >0.9999). (K) Representation of the average number of rewards obtained every minute across the 2-hour test PR2 session. (L) During Hargreaves test the paw withdrawal latency is slightly increased after U50,488 injection in the NAcShCS (two-way ANOVA for repeated measures: time $F_{2,28}$=9,246, p=0.0008; interaction $F_{2,28}$=4.060, p=0.0283; Post hoc test: aCSF (n=7) vs. U50,488 (n=7) on PR2: p=0.0326).

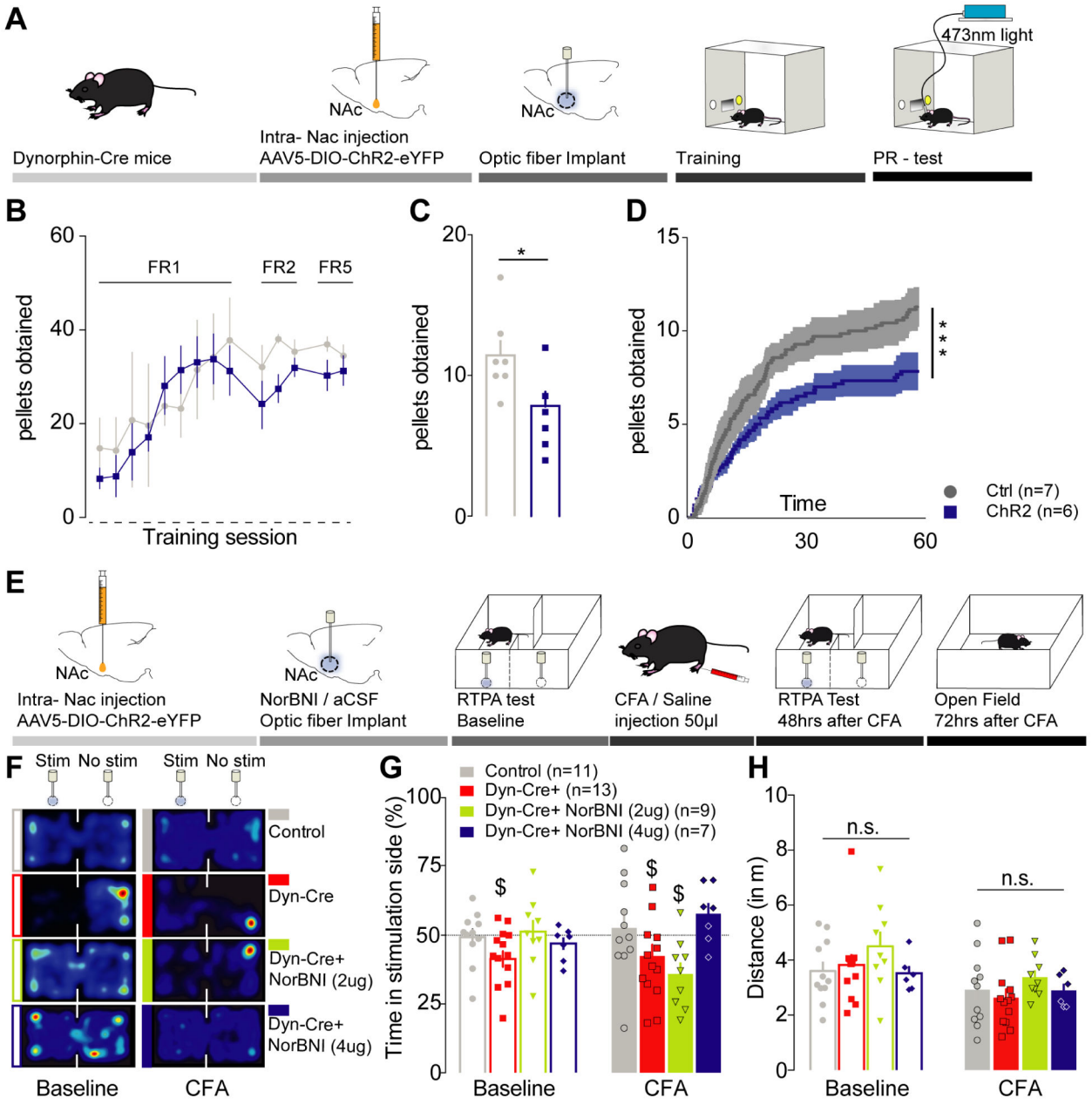

Figure 2: Activation of dynorphin-containing neurons in the vNACSh is sufficient to drive negative affective states and aversive behavior.

(A) Schematic representation of the behavioral paradigm. (B) Representation of training process across experimental days for mice. (C) Photo-stimulation of dynorphin-containing neurons in the vNAcSh is sufficient to decrease motivation for sucrose self-administration (Mann-Whitney: Ctrl (n=7) vs Chr2 (n=6), p=0.0385). (D) Representation of the average number of rewards obtained every minute across the 1-hour test session (Kolgomorov-Smirnov: p<0.0001). (E) Schematic representation of the behavioral paradigm for real time place preference testing (RTPT). (F) Representative heat maps of the animal activity during the 20 minutes RTPT. (G) During baseline test (no pain) aCSF-dyn-cre+ mice demonstrated an aversion for the photo-stimulated compartment (one sample t-test compared to 50%:

n=13, p=0.0352). This effect was fully prevented by norBNI pre-treatment (one sample t-test compared to 50%: norBNI-dyn-cre+ 2μg: n=9, p=0.6833, norBNI-dyn-cre+ 4μg: n=7, p=0.3014). Two days after pain induction, 2μg of norBNI did not reverse the aversive properties of dynorphin-containing neurons stimulation (one sample t-test compared to 50%: n=9, p=0.0122). In contrast 4μg of norBNI successfully prevented photo-stimulation induced aversion (one sample t-test compared to 50%: n=7, p=0.0807). (H) Locomotor activity was similar throughout all groups of mice during RTPT (two-way ANOVA for repeated measures: time: $F_{1, 33} = 30.16$, $p<0.0001$; treatment: $F_{3, 33}= 0.7857$, $p= 0.5105$; interaction: $F_{3, 33} = 1.342$, $p=0.5722$).

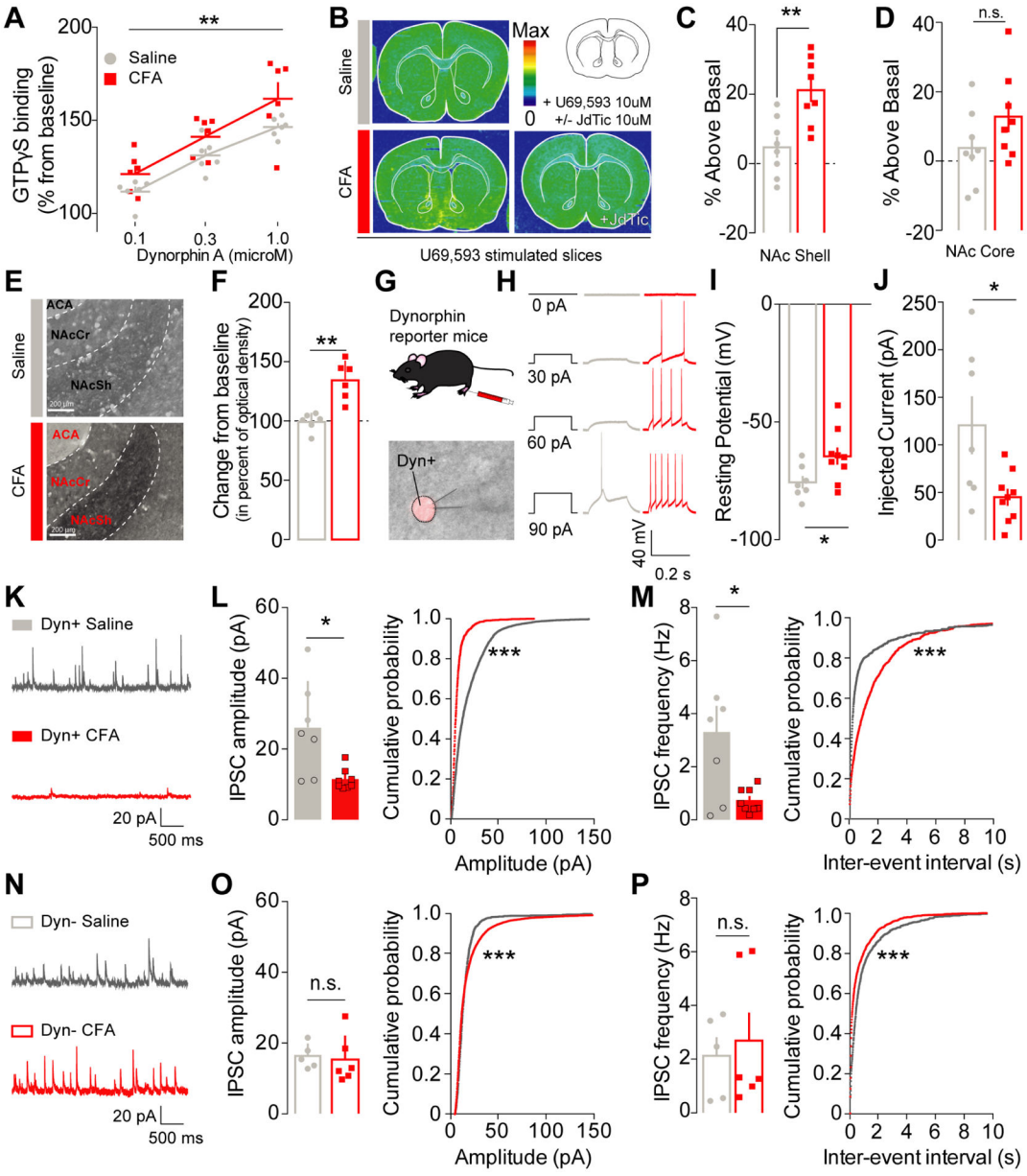

Figure 3: Inflammatory pain increases KOR functional activity and recruits dynorphin-containing neurons in the NAcShell through a disinhibition mechanism.

(A) Dynorphin A stimulation dose-dependently increases GTPγS incorporation in NAc tissue from CFA- (n=6) and saline-injected rats (n=6) (two-way mixed-model ANOVA: dose: $F_{1, 30}$= 8.717, p=0.0066). GTPγS incorporation is significantly higher in CFA-treated animals suggesting an increase in KOR functional activity (two-way mixed-model ANOVA: pain effect: $F_{2, 30}$ = 29.98, p<0.0001). (B) Representative GTPγS autoradiography of slices incubated with U69,593 in saline (top) and CFA +/− JdTic (bottom) injected animals. (C) In conditions of pain, KOR functional activity was increased in the NAc shell (unpaired two-way t-test: p=0.0027, n=8). (D) but not in the NAc core (unpaired two-way t-test: p=0.1450, n=8). (E) Representative pictures of dynorphin A expression in the NAcShCS in either saline (top) and CFA-injected animals (bottom). ACA: Anterior Commisure, NAcSh: Nucleus

Accumbens Shell; NAcCr: Nucleus Accumbens Core. (F) Dynorphin A content in the NAcShCS is increased after CFA-induced inflammation (Mann-Whitney test for unpaired values; p=0.0022, n=6). (G) Schematic representation of electrophysiology methodology. Lower panel : representative picture a patch pipet onto the somatic area of a Ai14+ dynorphin neuron in the vNACsh. (H) Representative traces of current-response from vNacSh dynorphin neurons obtained from either saline or CFA mice. (I) CFA-injected animals display a higher resting membrane potential (unpaired two-way t-test: p=0.032, $n_{cells/animals}$=7-9/4), and (J) a lower rheobase (unpaired two-way t-test: p=0.019, $n_{cells/animals}$=7-9/4). (K) Representative traces of sIPSCs from dyn+ neurons. (L) Amplitude and (M) frequency of sIPSC onto dyn+ neurons are decreased in conditions of inflammatory pain as compared to saline control (frequency: two–tailed t-test for unpaired values p=0.0406; amplitude: two-tailed Mann-Whitney for unpaired values p=0.0140, $n_{cells/animals}$=7-8/4). The cumulative probability plots demonstrate a significant shift towards smaller and less frequent events in dynorphin+ neurons after CFA (Kolmogorov-Smirnov test p<0.0001, $n_{cells/animals}$=7-8/4). (N) Representative traces of sIPSCs from Dyn- neurons. (O) Neither the mean amplitude or (P) frequency of sIPSCs onto dyn- neurons are affected by inflammatory pain (frequency: two-tailed Mann-Whitney for unpaired values p=0.6277; amplitude: two–tailed Mann-Whitney for unpaired values p=0.4242, $n_{cells/animals}$=5-6/4). A plot of the cumulative probability revealed a significant shift towards larger and more frequent events in dynorphin negative neurons after CFA (Kolmogorov-Smirnov test p<0.0001, $n_{cells/animals}$=5-6/4).

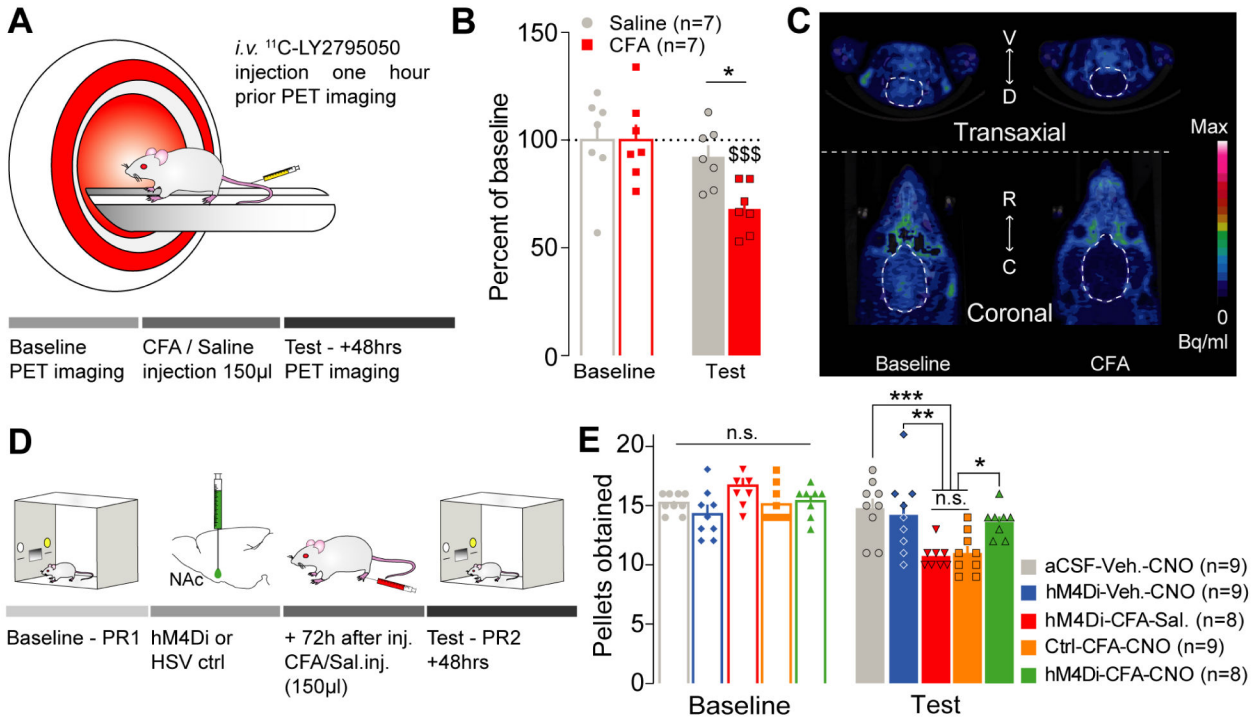

Figure 4: Inflammatory pain mediates negative affective states through recruitment of dynorphin-containing neurons in the NAcShCS.

(A) Schematic representation of the PET imaging methodology in rats. (B) Inflammatory pain, but not saline control, decreases the distribution volume of ^{11}C-LY2795050 observed in rat's brain two days after CFA injection (two-way ANOVA for repeated measures: time: $F_{1,12}$=26.88, p=0.0002; interaction: $F_{1,12}$=10.02, p=0.0081; post hoc tests: baseline CFA vs test CFA: p<0.0001; baseline saline vs test saline: p=0.3260; test CFA vs test saline: p=0.0282, n=7). (C) Representative images of PET imaging before (left) and after (right) inflammation. (D) Schematic representation of the behavioral methodology. (E) Silencing dynorphin neurons in the NAcShCS prevented the inflammatory pain-induced decrease in motivation for sucrose self-administration (two-way ANOVA for repeated measures: time: $F_{1, 38}$= 75.81, p<0.0001; interaction: $F_{4,38}$= 15.84, p<0.0001. Post-hoc test: aCSF-Veh.-CNO vs hM4Di-CFA-Sal.: p=0.0006; aCSF-Veh.-CNO vs Ctrl-CFA-CNO: p=0.0003; Ctrl-CFA-CNO vs. hM4Di-CFA-CNO: p=0.0255; hM4Di-CFA-Sal. vs hM4Di-CFA-CNO: p=0.0417; hM4Di-CFA-Sal. vs. hM4Di-Veh.-CNO: p=0.0046; Ctrl-CFA-CNO vs. hM4Di-Veh.-CNO: p= 0.0027; hM4Di-CFA-CNO vs. hM4Di-Veh.-CNO: p=0.9658; hM4Di-CFA-Sal. Vs Ctrl-CFA-CNO: p=0.9988; aCSF-Veh.-CNO vs. hM4Di-Veh.-CNO: p=0.9706; and aCSF-Veh.-CNO vs hM4Di-CFA-CNO: p=0.7173, n=8-9).